

## Numerical modeling of the magnetic topology near Mars auroral observations

M. W. Liemohn,<sup>1</sup> Y. Ma,<sup>2</sup> A. F. Nagy,<sup>1</sup> J. U. Kozyra,<sup>1</sup> J. D. Winningham,<sup>3</sup> R. A. Frahm,<sup>3</sup> J. R. Sharber,<sup>3</sup> S. Barabash,<sup>4</sup> and R. Lundin<sup>4</sup>

Received 29 August 2007; revised 30 October 2007; accepted 15 November 2007; published 22 December 2007.

[1] Magnetohydrodynamic (MHD) simulations of the Mars magnetic field topology are presented for the auroral observations reported from the Mars Express SPICAM instrument. It is found that the field lines closest to the assumed emission location are open. That is, they are connected to the interplanetary magnetic field, thus allowing access for solar wind electrons to bombard the upper atmosphere and create a auroral-like emission. The most likely population responsible for the creation of the emissions recorded by SPICAM is magnetosheath electrons. It is found that numerous closed magnetic field lines, connected to two strong crustal field regions, can straddle the terminator, leaving open the speculation that atmospheric photoelectrons could be responsible for nightside auroral-like emissions. However, for the particular case of the initially reported SPICAM auroral observations, the MHD results do not produce such terminator-crossing field lines near the emission region.

**Citation:** Liemohn, M. W., Y. Ma, A. F. Nagy, J. U. Kozyra, J. D. Winningham, R. A. Frahm, J. R. Sharber, S. Barabash, and R. Lundin (2007), Numerical modeling of the magnetic topology near Mars auroral observations, *Geophys. Res. Lett.*, *34*, L24202, doi:10.1029/2007GL031806.

### 1. Introduction

[2] *Bertaux et al.* [2005] noted the observation of a burst of aurora-like emission in the data from the Spectroscopy for Investigation of Characteristics of the Atmosphere of Mars (SPICAM) instrument [*Bertaux et al.*, 2006] on board the Mars Express (MEX) satellite [*Chicarro et al.*, 2004]. Near 0602 UT on August 11, 2004, as MEX was moving southward through the evening sector near its orbit periapsis, SPICAM measured an intense spike in the ultraviolet emissions from an atmospheric location above a strong, nearly vertical crustal magnetic field [e.g., *Acuña et al.*, 1999]. The inferred position of the emission was estimated to be near 178°E longitude and  $-50^\circ$  latitude (roughly 2100 local time). *Bertaux et al.* [2006] mention that other auroral-like emissions have since been identified in the SPICAM data set, all occurring over the strong crustal field region in

the southern hemisphere (F. Leblanc et al., unpublished manuscript, 2007).

[3] The original estimate of the emission region and characteristics led *Bertaux et al.* [2005] to infer that these emissions were caused by an electron energy source having a precipitating characteristic energy in the range of a few hundred eV (this is higher than typical magnetosheath electron energies [e.g., *Mitchell et al.*, 2001]) and a flux intensity around 10 times higher than typical magnetosheath fluxes. The assumption of a magnetosheath source implied an acceleration mechanism along the auroral field line.

[4] Observations of accelerated downflowing electrons at Mars have since been reported by *Lundin et al.* [2006a, 2006b] from the Analyzer of Space Plasmas and Energetic Atoms (ASPERA-3) electron spectrometer (ELS) instrument [*Barabash et al.*, 2006] on MEX as well as by *Brain et al.* [2006] with the electron reflectometer (ER) from Mars Global Surveyor (MGS) [*Acuña et al.*, 1992]. These measurements show acceleration of 100s of eV to several keV, often associated with the edges of the strong crustal field region and with weak crustal field regions near the equator.

[5] *Leblanc et al.* [2006], however, reanalyzed the data of *Bertaux et al.* [2005] and concluded that the emission region could have been much wider in extent than originally assumed. Their assessment of the data led to the conclusion that the auroral emissions were most likely from electrons with tens of eV in energy rather than hundreds or thousands of eV. This allows for the possibility of non-accelerated magnetosheath electrons or even atmospheric photoelectrons to be the energy source for the emissions. Non-accelerated magnetosheath electrons have been reported over strong, nearly vertical crustal fields on both the dayside [e.g., *Liemohn et al.*, 2003] and the nightside [e.g., *Mitchell et al.*, 2001], and this is a likely candidate for the precipitating particle source causing the observed emissions. An atmospheric photoelectron source would require a closed loop magnetic topology that either (a) straddles the terminator plane, with one footpoint in the dayside ionosphere and the other on the nightside, or (b) contains a high-altitude reservoir of trapped photoelectrons that are precipitating with an intensity sufficient to produce a detectable emission.

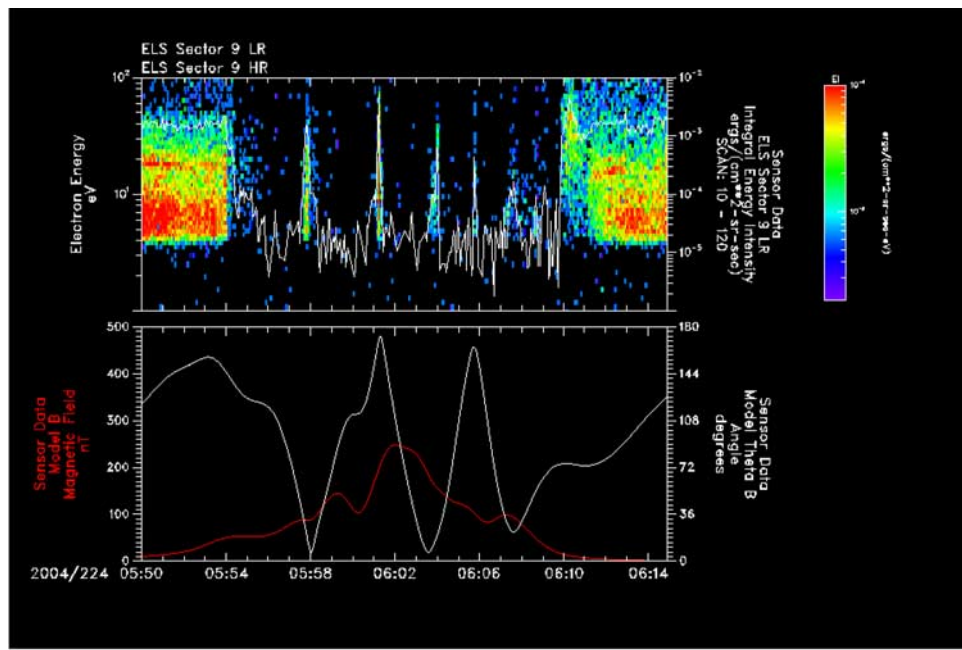
[6] The possibility that precipitating photoelectrons caused the auroral emissions gained traction when *Winningham et al.* [2005] reported ELS measurements of atmospheric photoelectron bursts during the MEX periapsis pass highlighted by *Bertaux et al.* [2005]. These are shown in Figure 1 (top) as the five isolated bursts of electrons from 0558 to 0607 UT (near periapsis) seen at times when the *Cain et al.* [2003] crustal field model predicts a nearly vertical magnetic orientation (Figure 1, middle). These electrons were determined to be atmospheric photoelectrons

<sup>1</sup>Atmospheric, Oceanic, and Space Sciences Department, University of Michigan, Ann Arbor, Michigan, USA.

<sup>2</sup>Institute for Geophysics and Planetary Physics, University of California, Los Angeles, California, USA.

<sup>3</sup>Southwest Research Institute, San Antonio, Texas, USA.

<sup>4</sup>Swedish Institute of Physics, Kiruna, Sweden.



MEX Data: 2004, DOY=224, UT=05:58

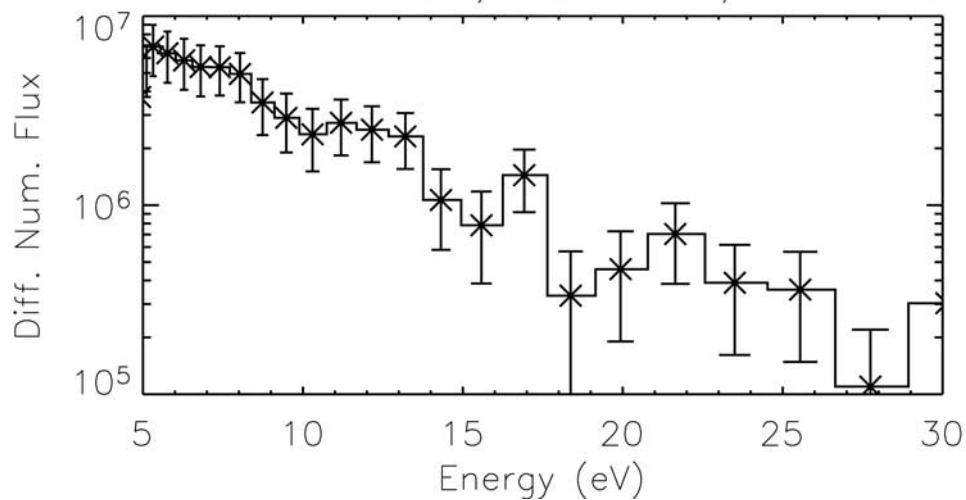


**Figure 1.** MEX ELS data for the interval near the SPICAM auroral emission observations. (top) Energy vs. time spectrogram from ELS and (middle) magnetic field elevation angle as computed from the *Cain et al.* [2003] crustal magnetic field model. (bottom) The energy spectrum for the burst at 0558 UT.

by their energy spectrum (Figure 1, bottom), in which the 20–30 eV  $\text{CO}_2$  primary production peaks are visible (the peaks are at 17 and 22 eV, implying a  $-5$  V spacecraft potential, a typical value for MEX [e.g., *Frahm et al.*, 2006]). In addition, these electrons peak in ELS sector 11, which was viewing toward the dayside at this time (i.e., streaming toward the nightside, in favor of topology (a) mentioned above).

[7] The question therefore remains unanswered regarding the source population for the intense auroral-like emissions seen by SPICAM on August 11, 2004. In particular, the source is either magnetosheath electrons from the solar wind or atmospheric photoelectrons from the dayside ionosphere. These two sources require very different magnetic topologies; the former requiring an open field line and the latter requiring a closed field line that straddles the terminator.

This study answers this question by examining global magnetohydrodynamic (MHD) simulation results of the field line configurations near the emission location.

## 2. Model

[8] The numerical tool employed for this study is the multi-species magnetohydrodynamic (MHD) model of *Ma et al.* [2004]. This code solves the ideal MHD equations, but with 4 separate continuity equations for  $\text{H}^+$ ,  $\text{O}^+$ ,  $\text{O}_2^+$ , and  $\text{CO}_2^+$ . The simulation domain extends from 100 km altitude to many Mars radii on a spherical grid with an altitude step size ranging from 10 to 600 km and an angular grid spacing from  $1.875^\circ$  to  $3.75^\circ$  (the grid is more highly resolved near the planet). Thermospheric values are taken from the *Bougher et al.* [2001] code, and crustal magnetic fields

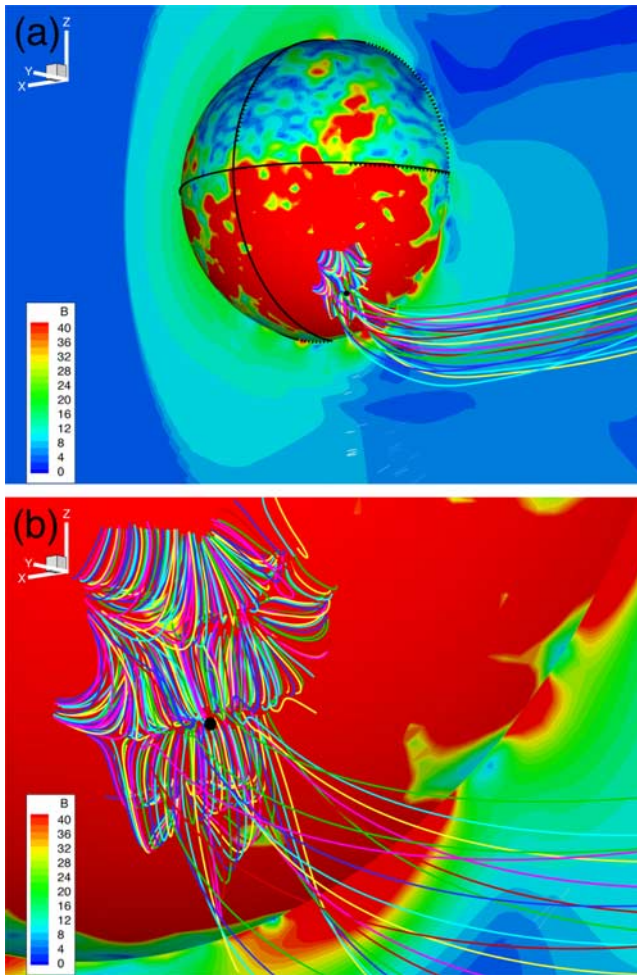


**Figure 2.** Magnetic field lines from the MHD simulation, centered on the location of the MEX SPICAM auroral emission. The field line traces were started at 200 km altitude in a  $1^\circ \times 1^\circ$  array. The color of the field lines is purely illustrative. The background color shows the magnetic field magnitude in the x-z plane and at the lower boundary of the simulation domain (i.e., 100 km altitude above Mars). The small black dot in the middle of the field lines marks the inferred location of the emissions. (a) A far-off view, with the sun to the left. (b) A close-up view. In Figure 2a, the “vertical” curved line on the sphere is the terminator and the “horizontal” curved line on the sphere is the equator.

are specified with the *Arkani-Hamed* [2002] model and included as a lower boundary condition.

[9] For the simulation discussed below, the upstream interplanetary magnetic field (IMF) and solar wind parameters were set to approximate the conditions during the SPICAM observations. The IMF is prescribed with a Parker spiral orientation ( $56^\circ$  offset from the  $-x$  axis in the  $+y$  direction,  $B_z = 0$ ) with a total IMF strength of 3 nT. The upstream solar wind is set to  $0.61 \text{ cm}^{-3}$  and 400 km/s. The density value is from an estimate of 0.81 nPa for the solar wind dynamic pressure, which is based on a magnetic pile-up region subsolar magnitude of 45 nT estimated from MGS measurements [e.g., *Crider et al.*, 2003]. The orien-

tation of the planet was set to a subsolar longitude of  $43^\circ\text{E}$ , so that  $178^\circ\text{E}$  is at 2100 local time (the place and time of the emission location). Solar minimum conditions are applied for the thermospheric and photoionization calculations in the MHD model.

[10] Magnetic field lines were then extracted from the MHD simulation results. Field lines are specified with a given starting location and then traced in each direction from that point. In the plots discussed below, magnetic field lines were extracted starting from either an array of points at a certain altitude or along the orbit path of the Mars Express satellite.

### 3. Results and Discussion

[11] The first set of field line extractions to be examined is the set of those around the auroral emission location. Figure 2 presents these results, from a viewpoint several Mars radii away (Figure 2a) and also a close-up view from just several hundred kilometers away (Figure 2b). Traces were begun at 200 km altitude in a dense grid in both longitude ( $125^\circ$  to  $145^\circ$  east of subsolar, i.e.,  $168^\circ\text{E}$  to  $188^\circ\text{E}$ ) and latitude ( $35^\circ$  to  $55^\circ\text{S}$ ). New starting points were taken every degree in this window, yielding 441 magnetic field line extractions. The view is from the evening sector, just below the equator. The color background shows the magnetic field intensity at 100 km altitude (on the sphere) and in the x-z plane. The colors of the individual field lines are arbitrarily chosen to ease the identification of each line. The SPICAM-inferred location of the intense emissions is very close to the center of the region of traced field lines.

[12] It is seen in Figure 2 that most of the extracted field lines are small closed loops that remain completely on the nightside of the planet (i.e., none crosses the terminator, the vertical black great circle on the sphere in Figure 2a). Several field lines extend tailward, eventually reaching the simulation boundary. That is, these are open field lines, connected to Mars at one end and to the IMF at the other. Figure 2b reveals an east-west row of open field lines through the middle of the extraction region, right where the emission location is inferred.

[13] How does this fit with the MEX ELS observations of photoelectrons streaming from the dayside at exactly the same time as the SPICAM emission observations? To answer this, field lines extractions were begun along the MEX satellite track during this interval. Figure 3 shows these traces, along with the MEX orbit track (yellow line) and the MEX location during the ELS photoelectron bursts and the SPICAM auroral measurements (the various symbols on the orbit track). Many of the field lines are small closed loops on which the MEX orbit track is very near the apex. It is seen that several field lines associated with the photoelectron bursts, however, come very close to crossing the terminator, reaching the 100 km altitude stopping point of the trace within a few degrees of the  $y = 0$  plane (the black vertical great circle). The photoelectrons observed on these field lines therefore came from the lines’ conjugate ionospheric footpoints. There are several open field lines connected to the planet and to the IMF, but these are very few and not coincident with the electron burst observations. It is also seen in Figure 3, however, that none of the



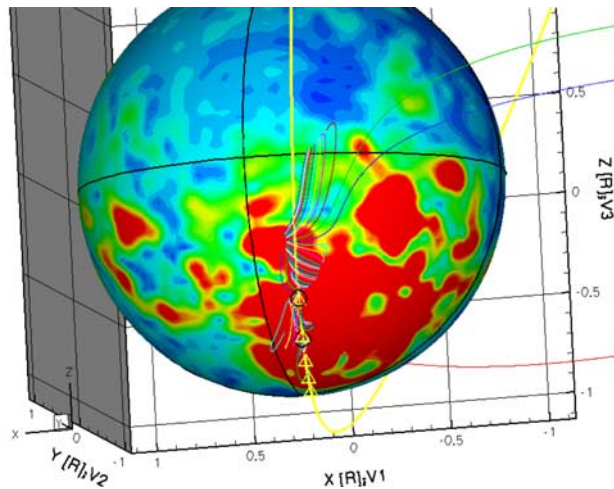


**Figure 3.** Field lines extracted along the Mars Express orbit track (the yellow line) during this periapsis pass. The triangle markers are places where ELS observed a burst of photoelectrons coming from the dayside direction, the upper black circle is the burst spectrum shown in Figure 1, and the lower black circle is the MEX location during the SPICAM auroral emission observations.

extracted field lines connect to the inferred location of the auroral emissions ( $\sim 10\text{--}15^\circ$  east of the orbit track).

[14] To assess the relative frequency of terminator-straddling field lines, several other field line extractions were conducted. The resulting traces are shown in Figure 4. Figure 4a are traces starting at 600 km altitude above Mars in a  $5^\circ$  by  $5^\circ$  longitude-latitude grid centered on the inferred emission location (extractions were taken from  $158^\circ$  to  $198^\circ\text{E}$  longitude and  $20^\circ$  to  $60^\circ\text{S}$  latitude, 81 extractions total). It is seen that there are some closed loops and quite a few open field lines, but no terminator-straddling loops (open or closed). Most of the closed field lines are below this altitude, and therefore the extraction favors the field lines originating in the cusp regions and yields a relatively large number of open field lines (compared to Figure 2).

[15] Figure 4b is a similar field line extraction (starting points at 600 km altitude every  $5^\circ$ ), except that the starting grid is shifted in longitude to overlap the terminator (the grid extends from  $123^\circ$  to  $163^\circ\text{E}$  longitude, and the terminator is at  $133^\circ\text{E}$  longitude). This figure reveals numerous closed loops that straddle the terminator. While most of these are small, localized loops, some are lengthy field lines that extend hundreds of kilometers on one or both sides of the terminator. There are fewer open field lines from this starting grid than the one used for Figure 4a. Several are open towards the dayside, crossing in front of Mars (through the magnetic pile-up region) and eventually crossing the magnetic pile-up boundary (MPB) and the bow shock on the dawnside flank.

[16] Figure 4c shows a final extraction, with the starting points shifted in longitude and latitude to the subsolar region ( $\pm 20^\circ$  in each direction). This is a region of weak crustal field, yet it still reveals a substantial number of closed loops. About 10% of the field line traces show open field lines that cross the terminator on the dusk side of the planet. These open field lines contain atmospheric photo-

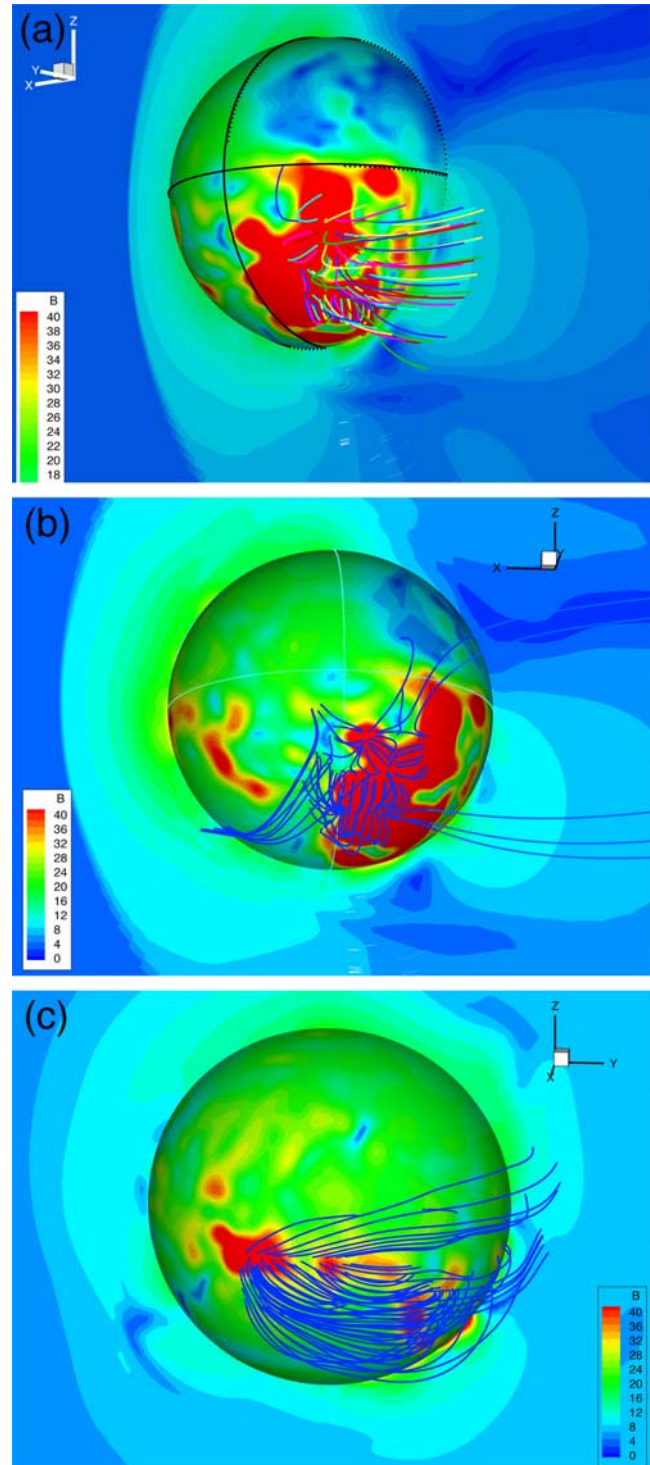


**Figure 4.** Magnetic field from the MHD simulation, extracted from 3 regions of the planet. All three plots show traces that started at 600 km altitude in a  $5^\circ \times 5^\circ$  array of starting locations. The extractions are from (a) the strong crustal field region where the auroral emissions were observed; (b) just nightside of the terminator, just west of the auroral emission location; and (c) the dayside equatorial region.

electrons and have been examined by *Frahm et al.* [2006, 2007] and *Liemohn et al.* [2006, 2007]. Another 10% of the extracted field lines are closed and connected to crustal field regions very close to the terminator. While none of the extracted field lines connect from the dayside subsolar region to the evening sector, the extraction reveals related magnetic topologies: (1) closed very close to the evening terminator and (2) open yet draped right over the evening sector. The existence of field lines extending from the dayside ionosphere, across the terminator and connected to Mars on the nightside of the planet is, therefore, a distinct and likely possibility.

[17] A few caveats to this study should be mentioned. One is that a numerical sensitivity check was not presented. Furthermore, MHD simulation results with idealized input conditions were examined, and the results could be significantly different during the passage of transient solar wind disturbances. Such issues will be examined in a future study.

#### 4. Conclusion

[18] This study examined the issue of magnetic field line topology around the location of the Mars Express SPICAM observations of auroral emissions. The question being addressed was whether the auroral field lines were closed loops, requiring an ionospheric energy source, or open lines connected to the solar wind IMF. If closed, especially if closed along a line straddling the terminator plane, then the auroral energy source is most likely atmospheric photoelectrons from the conjugate ionosphere. If open, then the auroral energy source is most likely solar wind/magneto-sheath electrons precipitating from interplanetary space.

[19] MHD simulation results were examined to assess the magnetic topology for this scenario. It was concluded that the auroral emission location is connected to open magnetic field lines, implying a solar wind electron energy source. However, field line traces from elsewhere around Mars show that some magnetic field lines do straddle the terminator, allowing for the possibility of photoelectron-induced auroral emissions at Mars. The two MEX observations are, therefore, not in contradiction. The differences between these two measurements can be explained with an analysis of the magnetic topology from an MHD simulation of this scenario. Both solar wind electrons and atmospheric photoelectrons can reach the nightside thermosphere and therefore both have the potential for creating auroral emissions at Mars.

[20] **Acknowledgments.** The authors would like to thank support for this research by NASA under grants NNG04GH60G, NASW-00003, NNG04G055G, and NNX07AN98G.

#### References

Acuña, M. H., et al. (1992), Mars Observer magnetic fields investigation, *J. Geophys. Res.*, *97*, 7799.  
 Acuña, M. H., et al. (1999), Global distribution of crustal magnetization discovered by the Mars Global Surveyor MAG/ER experiment, *Science*, *284*, 790.  
 Arkani-Hamed, J. (2002), An improved 50-degree spherical harmonic model of the magnetic field of Mars derived from both high-altitude

and low-altitude data, *J. Geophys. Res.*, *107*(E10), 5083, doi:10.1029/2001JE001835.  
 Barabash, S., et al. (2006), The Analyzer of Space Plasmas and Energetic Atoms (ASPERA-3) for the Mars Express mission, *Space Sci. Rev.*, *126*, 113, doi:10.1007/s11214-006-9124-8.  
 Bertaux, J.-L., et al. (2005), Discovery of an aurora on Mars, *Nature*, *435*, 790, doi:10.1038/nature03603.  
 Bertaux, J.-L., et al. (2006), SPICAM on Mars Express: Observing modes and overview of UV spectrometer data and scientific results, *J. Geophys. Res.*, *111*, E10S90, doi:10.1029/2006JE002690.  
 Bougher, S. W., S. Engel, D. P. Hinson, and J. M. Forbes (2001), Mars Global Surveyor electron density profiles: Neutral atmosphere implications, *Geophys. Res. Lett.*, *28*, 3091.  
 Brain, D. A., J. S. Halekas, L. M. Petcolas, R. P. Lin, J. G. Luhmann, D. L. Mitchell, G. T. Delory, S. W. Bougher, M. H. Acuña, and H. Rème (2006), On the origin of aurorae on Mars, *Geophys. Res. Lett.*, *33*, L01201, doi:10.1029/2005GL024782.  
 Cain, J. C., B. B. Ferguson, and D. Mozzoni (2003), An  $n = 90$  internal potential function of the Martian crustal magnetic field, *J. Geophys. Res.*, *108*(E2), 5008, doi:10.1029/2000JE001487.  
 Chicarro, A., P. Martin, and R. Trautner (2004), The Mars Express mission: An overview, in *Mars Express: The Scientific Payload, ESA Spec. Publ.*, vol. SP-1240, edited by A. Wilson, pp. 3–13, ESA Publ. Div., Noordwijk, Netherlands.  
 Crider, D. H., D. Vignes, A. M. Krymskii, T. K. Breus, N. F. Ness, D. L. Mitchell, J. A. Slavin, and M. H. Acuña (2003), A proxy for determining solar wind dynamic pressure at Mars using Mars Global Surveyor data, *J. Geophys. Res.*, *108*(A12), 1461, doi:10.1029/2003JA009875.  
 Frahm, R. A., et al. (2006), Carbon dioxide photoelectron peaks at Mars, *Icarus*, *182*, 371, doi:10.1016/j.icarus.2006.01.014.  
 Frahm, R., et al. (2007), Locations of atmospheric photoelectron energy peaks within the Mars environment, *Space Sci. Rev.*, *126*, 389.  
 Leblanc, F., O. Witasse, J. Winningham, D. Brain, J. Lilensten, P.-L. Blelly, R. A. Frahm, J. S. Halekas, and J. L. Bertaux (2006), Origins of the Martian aurora observed by Spectroscopy for Investigation of Characteristics of the Atmosphere of Mars (SPICAM) on board Mars Express, *J. Geophys. Res.*, *111*, A09313, doi:10.1029/2006JA011763.  
 Liemohn, M. W., D. L. Mitchell, A. F. Nagy, J. L. Fox, T. W. Reimer, and Y. Ma (2003), Comparisons of electron fluxes measured in the crustal fields at Mars by the MGS magnetometer/electron reflectometer instrument with a  $B$  field-dependent transport code, *J. Geophys. Res.*, *108*(E12), 5134, doi:10.1029/2003JE002158.  
 Liemohn, M. W., et al. (2006), Numerical interpretation of high-altitude photoelectron observations, *Icarus*, *182*, 383.  
 Liemohn, M. W., et al. (2007), Mars global MHD predictions of magnetic connectivity between the dayside ionosphere and the magnetospheric flanks, *Space Sci. Rev.*, *126*, 63.  
 Lundin, R., et al. (2006a), Plasma acceleration above Martian magnetic anomalies, *Science*, *311*, 980.  
 Lundin, R., et al. (2006b), Ionospheric plasma acceleration at Mars: ASPERA-3 results, *Icarus*, *182*, 308.  
 Ma, Y., A. F. Nagy, I. V. Sokolov, and K. C. Hansen (2004), Three-dimensional, multispecies, high spatial resolution MHD studies of the solar wind interaction with Mars, *J. Geophys. Res.*, *109*, A07211, doi:10.1029/2003JA010367.  
 Mitchell, D. L., R. P. Lin, C. Mazelle, H. Rème, P. A. Cloutier, J. E. P. Connerney, M. H. Acuña, and N. F. Ness (2001), Probing Mars' crustal magnetic field and ionosphere with the MGS Electron Reflectometer, *J. Geophys. Res.*, *106*, 23,419.  
 Winningham, J. D., et al. (2005), Electron observations near "Martian Aurora," *Eos Trans. AGU*, *86*(52), Fall Meet. Suppl., Abstract SH42A-03.

S. Barabash and R. Lundin, Swedish Institute of Physics, Box 812, Kiruna SE-981 28, Sweden.

R. A. Frahm, J. R. Sharber, and J. D. Winningham, Southwest Research Institute, P.O. Drawer 28510, San Antonio, TX 78228, USA.

J. U. Kozyra, M. W. Liemohn, and A. F. Nagy, Atmospheric, Oceanic, and Space Sciences Department, University of Michigan, 2455 Hayward Street, Ann Arbor, MI 48109-2143, USA. (liemohn@umich.edu)

Y. Ma, Institute for Geophysics and Planetary Physics, University of California, Los Angeles, 6877 Slichter Hall, Los Angeles, CA 90095, USA.